

RESEARCH

Open Access



MdNup62 interactions with MdHSFs involved in flowering and heat-stress tolerance in apple

Chenguang Zhang[†], Na An[†], Peng Jia[†], Wei Zhang, Jiayan Liang, Hua Zhou, Dong Zhang, Juanjuan Ma, Caiping Zhao, Mingyu Han, Xiaolin Ren and Libo Xing^{*}

Abstract

Because of global warming, the apple flowering period is occurring significantly earlier, increasing the probability and degree of freezing injury. Moreover, extreme hot weather has also seriously affected the development of apple industry. Nuclear pore complexes (NPCs) are main channels controlling nucleocytoplasmic transport, but their roles in regulating plant development and stress responses are still unknown. Here, we analysed the components of the apple NPC and found that MdNup62 interacts with MdNup54, forming the central NPC channel. MdNup62 was localized to the nuclear pore, and its expression was significantly up-regulated in 'Nagafu No. 2' tissue-cultured seedlings subjected to heat treatments. To determine *MdNup62*'s function, we obtained *MdNup62*-overexpressed (OE) Arabidopsis and tomato lines that showed significantly reduced high-temperature resistance. Additionally, OE-*MdNup62* Arabidopsis lines showed significantly earlier flowering compared with wild-type. Furthermore, we identified 62 putative MdNup62-interacting proteins and confirmed MdNup62 interactions with multiple MdHSFs. The OE-*MdHSFA1d* and OE-*MdHSFA9b* Arabidopsis lines also showed significantly earlier flowering phenotypes than wild-type, but had enhanced high-temperature resistance levels. Thus, MdNUP62 interacts with multiple MdHSFs during nucleocytoplasmic transport to regulate flowering and heat resistance in apple. The data provide a new theoretical reference for managing the impact of global warming on the apple industry.

Keywords: Apple, Flowering, Heat stress, Nuclear pore complex, *MdNup62*, *MdHSFs*

Introduction

Apple (*Malus × domestica* Borkh.) is a widely cultivated and economically important fruit crop in temperate regions worldwide owing to its high nutritional value, good storage, and lengthy supply period. And Fuji apple is the main cultivar in China, but there are cultivation and production problems, including flowering difficulties and severe alternate bearing [1, 2]. However, with global

warming, an increase in the average temperature in winter will result in earlier apple flowering [3, 4], and if there is cold weather in early spring, then significant flower and fruit losses will result. Additionally, at present, extreme hot weather occurs frequently in summer, causing other problems, such as growth impairment and production decline [5, 6], which have seriously affected the development of the apple industry in China.

Floral induction pathways have been extensively studied, and there are six signalling pathways in the model plant *Arabidopsis thaliana*, including photoperiodic, vernalization, autonomic, gibberellin, temperature-sensitive, and age pathways[7–9]. In apple, the functions of some key flowering-related genes have been well studied in

[†]Chenguang Zhang, Na An and Peng Jia contributed equally to this work.

^{*}Correspondence: libo_xing@nwsuaf.edu.cn

College of Horticulture, Northwest A&F University, 3 Taicheng Road, Yangling, 712100 Shaanxi, China



recent years, such as *APETALA1* (*API*), *LEAFY* (*LFY*), *FLOWERING LOCUS T* (*FT*), and *TERMINAL FLOWER 1* (*TFL1*). For instance, overexpression of *MdMADS5*, a putative homolog of *API*, leads to significant early flowering in Arabidopsis [10]. Apple anti-*TERMINAL FLOWER 1* transgenic lines flower significantly earlier than the WT, with the earliest flowering at 8 months, while the WT did not flower for 6 years [11]. Through transcriptome analyses, the induction of apple flower buds was found to be regulated by sugar and hormone signalling pathways [12]. Other omics studies have revealed the molecular mechanisms involved in responses to exogenous treatments, such as sugar [13], 6-benzylaminopurine [14], and gibberellins [15], and their effects on the flowering of apples. However, research on apple flowering is still relatively limited.

A nuclear pore complex (NPC) is composed of a class of nucleoporins (Nups) located in the nuclear pore [16]. More than 30 Nups have been identified in Arabidopsis and 38 members have been identified in apple [16, 17]. Some Nups interact and form three subcomplexes: Nup62, Nup93, and Nup107–160 [16, 18]. Nups control the transport of substances, such as RNA and proteins, between the nucleus and cytoplasm [19, 20], and play important roles in regulating plant growth and development, as well as biotic and abiotic stresses [19, 21, 22]. For example, *HOS1*, *Nup96*, *Nup54*, *Nup58*, *Nup62*, *Nup136*, and *Nup160* are important for plant flowering [16, 23–26]. *HOS1*, *Nup85*, *Nup96*, and *Nup133* participate in abiotic stress pathways [18, 20, 27–29]. *MOS7*, *Nup96*, *Nup160*, and *Sec1* play important roles in plant immunity [30–32], and *Nup96*, *Nup160*, and *TPR* affect hormone signalling pathways [33–37].

Heat shock factors (*HSFs*) are important components of signal transduction and play important roles in diverse stress pathways [38]. The *HSF* family in plants has more members (21 *HSFs* in *Arabidopsis*) and more complex regulatory mechanisms [39, 40] than in vertebrates (4 *HSFs*) or *Drosophila* (only 1 *HSF*). On the basis of their structural differences, *HSFs* may be divided into three classes, A, B, and C [39]. Class A has the C-terminal short peptide AHA domain, which has an activator function, while the B and C classes lack this domain [41]. *HSFs* specifically identify and bind heat shock elements (HSEs), which contain nGAAnnTTCn or nTTCnnGAAn in the downstream target genes' promoters [42]. Class A members (*HSEA1a*, *HSEA1b*, *HSEA1d*, *HSEA1e*, *HSEA2*, and *HSEA3*) positively regulate plant heat tolerance [43–47], while, in contrast, Class B *HSFs* (*HSFB1* and *HSFB2b*) negatively regulate heat-induced *HSFs* and plant heat tolerance [48]. In addition to responding to heat stress, some *HSFs* (*HSEA2*, *HSEA1E*, and *HSEA4C*) appear to be involved in plant flowering pathways [49, 50].

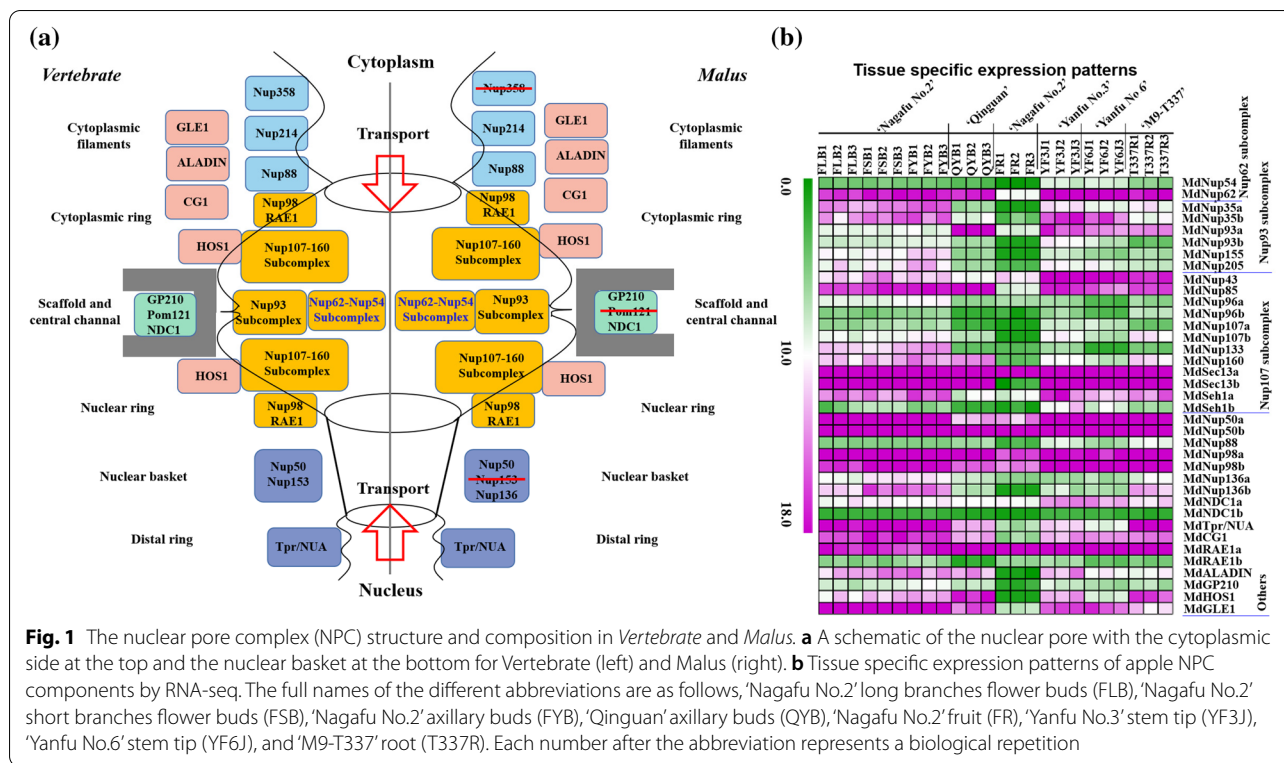
Currently, there are no reported functional studies of Nups in apple. *Nup62* is a member of the Nup62 subcomplex in the central core of the nuclear pore [16, 17], and *nup62 A. thaliana* mutants have been reported to flower early, indicating *Nup62*'s involvement in flowering pathways [25]. In this study, we characterized apple *Nup62*, which showed a high transcription level at the flower bud developmental stage and was responded to high temperature. The overexpression of *MdNup62* in Arabidopsis resulted in earlier flowering compared with WT. Moreover, The overexpression of *MdNup62* in Arabidopsis and tomato both reduced heat resistance. Further, we performed a yeast two-hybrid (Y2H) sieve library experiment to screen for proteins that interact with *MdNup62*, and the interactions between *MdNup62* and the *MdHSFs* were confirmed. And the overexpression of *MdHSEA1d* and *MdHSEA9b* independently in Arabidopsis resulted in earlier flowering and enhancing heat resistance. Thus, *MdNup62* and the *MdHSFs* regulate flowering and respond to temperature changes. These results provide a theoretical reference for managing the impact of global warming on the apple industry.

Results

Apple NPC structure and composition, and its expression patterns

Compared with vertebrate, apple NPC consists of 38 Nup proteins, but missing some Nups, such as Nup153, Nup358, Pom121, etc. Refer to the structure of vertebrate NPC [16], we divided apple NPC into five parts: Cytoplasmic filaments (Nup214 and Nup88), Cytoplasmic and Nuclear ring (Nup98, RAE1, and Nup107-160 Subcomplex), Scaffold and central channel (GP210, NDC1, Nup62 Subcomplex, and Nup93 Subcomplex), Nuclear basket (Nup50 and Nup136), and Distal ring (Tpr/NUA), as well as GLE1, ALADIN, CG1, and *HOS1* also participate in NPC constitution (Fig. 1a). Additionally, *MdNup62* interacts with *MdNup54* on Y2H and LUC experiment, and they might forming the central apple NPC channel involving in nucleocytoplasmic transport (Fig. S1) [17].

We examined the expression patterns of NPC components in different tissues of several apple varieties (Fig. 1b; Table S1). The expression levels of *MdNup62* as central channel component showed significantly higher in buds, stem, roots than in fruit of apples, but other channel component *MdNup54* showed significantly low expression levels in all tissues compared with *MdNup62*, indicating that *MdNup62* play a key role in regulation of growth and stress response by controlling nucleocytoplasmic transport in apple.



Feature, expression, and subcellular localization analyses of *MdNup62*

We initially performed a simple bioinformatics analysis of *MdNup62*. A phylogenetic tree of *Nup62* from six Rosaceae plants (*Rosa chinensis*, *Pyrus communis*, *Prunus persica*, *M. domestica*, *Rubus occidentalis*, and *Fragaria vesca*) was constructed using MEGA-X. *MdNup62* was most closely related to the *Nup62* of pear (Fig. 2a). The aligned protein sequences revealed a conserved Nsp1_C domain (Fig. 2b). The subcellular localization of *MdNup62* was determined by introducing 35S::*MdNup62*-GFP into tobacco leaves (Fig. 2c). Tobacco leaves transformed with the empty vector 35S::GFP were used as controls. In the tobacco leaves expressing 35S::*MdNup62*-GFP, the GFP signal was observed only in the nuclear pore, while the GFP signal was detected throughout the control tobacco leaf cells, indicating that *MdNup62* localized to the nuclear pore.

The transcript levels of *MdNup62* in different tissues were determined using qRT-PCR (Fig. 2d). The highest expression level was in flower buds. An *MdNup62* expression analysis during the flower bud developmental stages revealed that the expression level was stable at 30 to 60 days after flowering and reached its highest level at 70 days after flowering (Fig. 2e). Thus, *MdNup62* maintained a high expression level during

flower bud induction, indicating that it may be related to bud differentiation in apple.

We exposed apple tissue-cultured seedlings to a heat treatment. The reactive oxygen species (ROS) accumulation in leaves increased from 0 to 6 h under heat-treatment conditions (Fig. 2f). Moreover, the expression level of *MdNup62* was determined at different times during the high-temperature treatment (Fig. 2g). *MdNup62* was significantly induced by high temperature, and its expression level was highest at 1 h after exposure to the high temperature. Thus, *MdNup62* may be involved in the heat-resistance pathway of apple.

Overexpression of *MdNup62* promotes flowering

To confirm *MdNup62*'s role in flowering, we performed an Agrobacterium-mediated genetic transformation of *MdNup62* into *A. thaliana*. We found that OE-*MdNup62* lines flowered significantly earlier than WT (Fig. 3a). Additionally, OE-*MdNup62* lines had significantly fewer rosette leaves than WT during bolting (Fig. 3b). The presence of the transgene in OE-*MdNup62* lines was confirmed using genomic PCR (Figure S2a), semi-quantitative RT-PCR (Fig. 3c), and qRT-PCR (Fig. 3d). The transcript levels of flowering-related genes were analysed by qRT-PCR (Fig. 3e). The expression levels of *AtFT*, *AtLFY*, and *AtAPI* significantly increased in OE-*MdNup62* lines compared with WT. This demonstrated

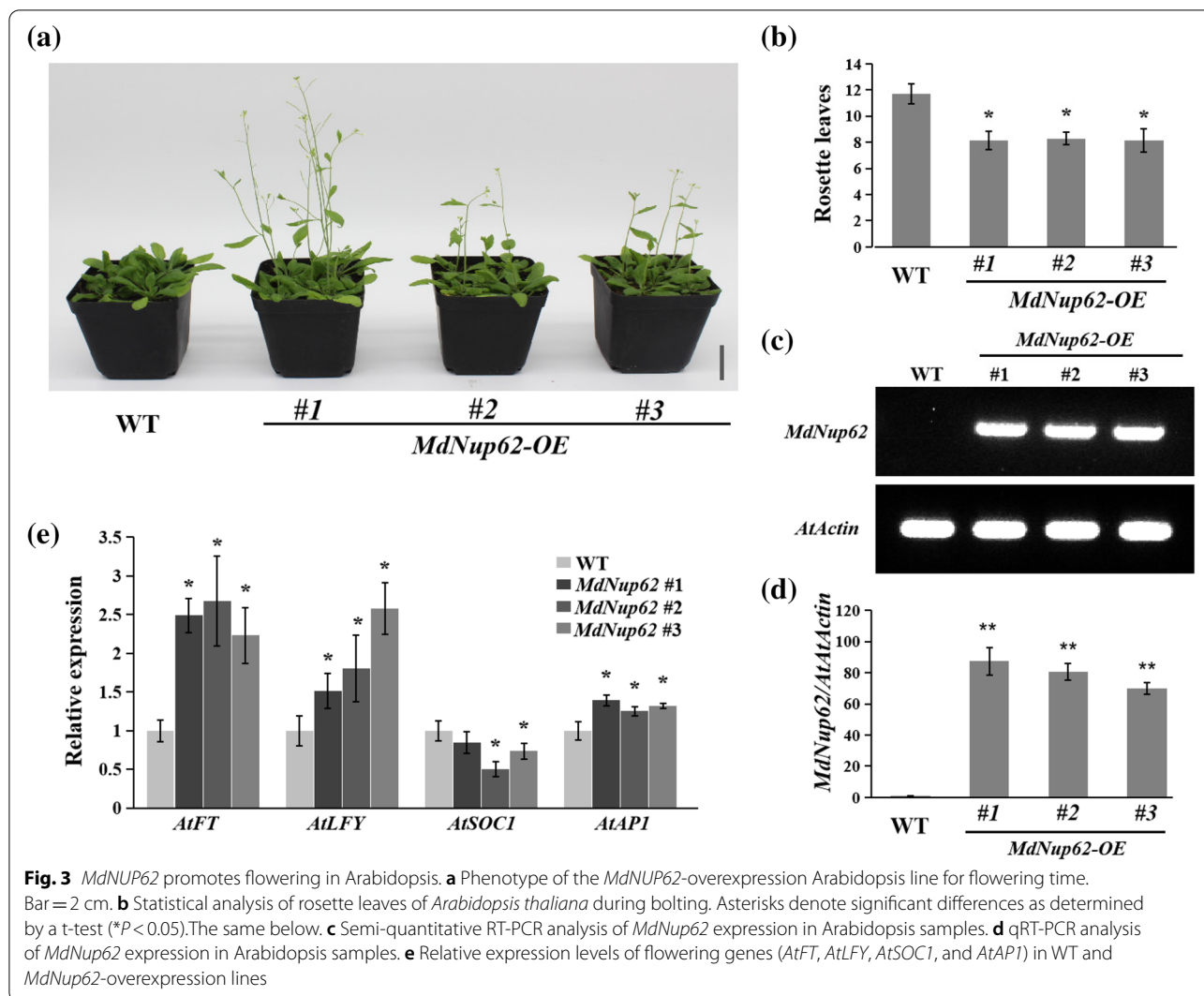


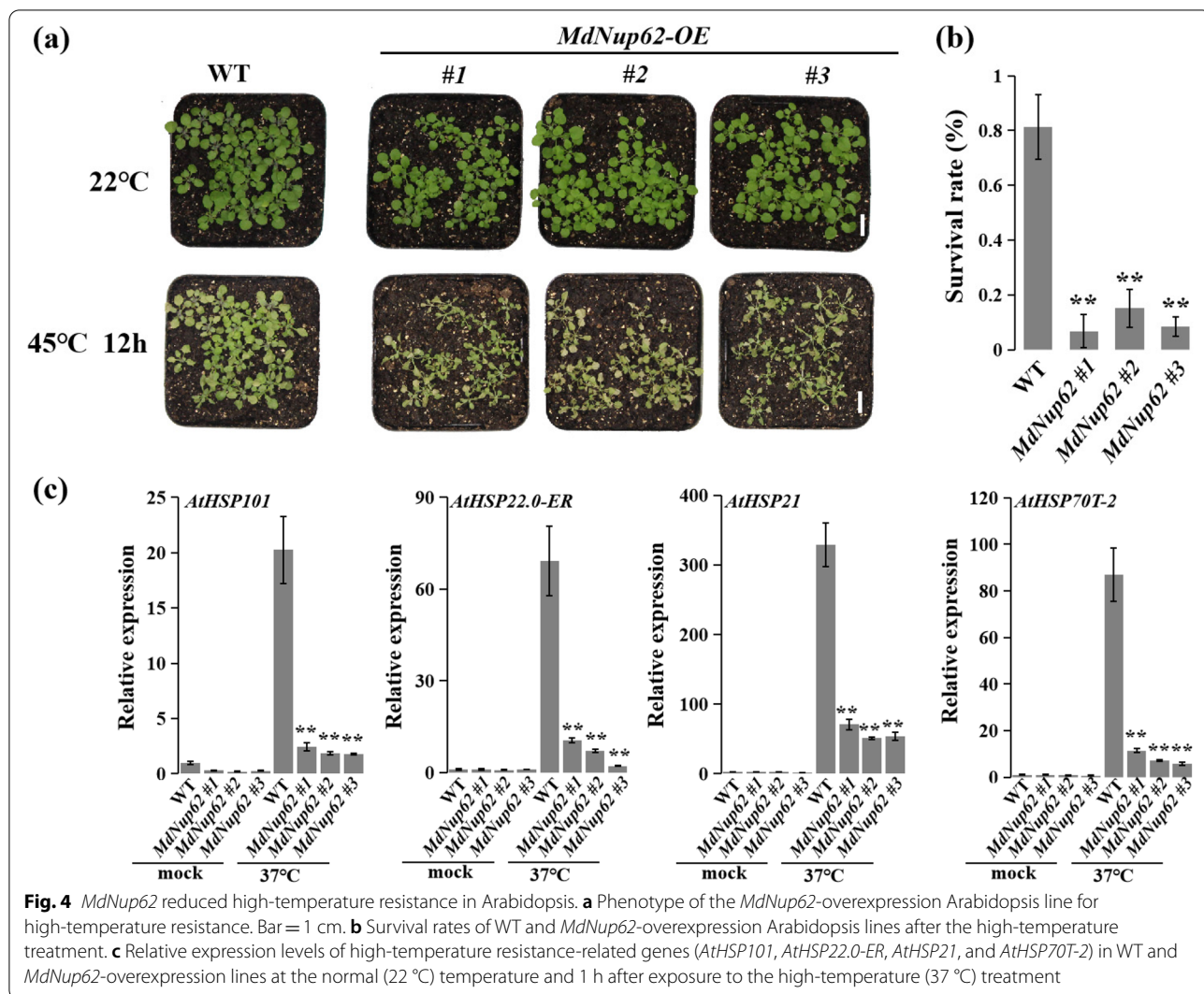
Fig. 3 *MdNUP62* promotes flowering in Arabidopsis. **a** Phenotype of the *MdNUP62*-overexpression Arabidopsis line for flowering time. Bar = 2 cm. **b** Statistical analysis of rosette leaves of *Arabidopsis thaliana* during bolting. Asterisks denote significant differences as determined by a t-test ($*P < 0.05$). The same below. **c** Semi-quantitative RT-PCR analysis of *MdNup62* expression in Arabidopsis samples. **d** qRT-PCR analysis of *MdNup62* expression in Arabidopsis samples. **e** Relative expression levels of flowering genes (*AtFT*, *AtLFY*, *AtSOC1*, and *AtAPI*) in WT and *MdNup62*-overexpression lines

the heat treatment, the ROS accumulation in leaves was clear greater in OE-*MdNup62* lines compared with WT (Fig. 5a). In addition, the malondialdehyde and H_2O_2 levels were significantly greater than in WT (Fig. 5b, c). Moreover, the superoxide dismutase, peroxidase, and catalase activities were lower in OE-*MdNup62* lines than in WT (Fig. 5d–f). High-temperature resistance assays were carried out in transgenic tomato plants (Fig. 6a). As in transgenic *A. thaliana*, the survival rate of transgenic tomato was significantly reduced compared with WT (Fig. 6b). The presence of the transgene in OE-*MdNup62* lines was confirmed by genomic PCR, and qRT-PCR (Fig. 6c,d). The expression levels of *HSPs* (*HSP101*, *HSP22-ER*, *HSP21.0*, and *HSP70T-2*) in transgenic tomato were significantly reduced under high-temperature conditions compared with under normal growth conditions (Fig. 6e). These

results indicate that *MdNup62* reduces plant high-temperature resistance.

MdNup62-interacting protein screening

To further reveal the function of *MdNup62*, we conducted a Y2H sieve library experiment using a *MdNup62* truncated body (*MdNup62*^{508–613}-pGBKT7) that is not self-activated. We identified 62 putative *MdNup62*-interacting proteins (Table S3). Some transcription factors were identified, such as HSFs (MdHSEA1d, MdHSEA1e, MdHSEA9, MdHSF30, MdHSF1, and MdHSF8), as well as MdMYB21, MdMYC2, MdGATA11, and MdBAK1. In addition, some enzymes and other functional genes were found. Because transcription factors that have transcriptional regulatory functions must be transported into the nucleus, and because *MdNup62* has regulatory effects on the transport of the proteins, we hypothesized that



MdNup62 interacts with these *MdHSFs* and controls their transport.

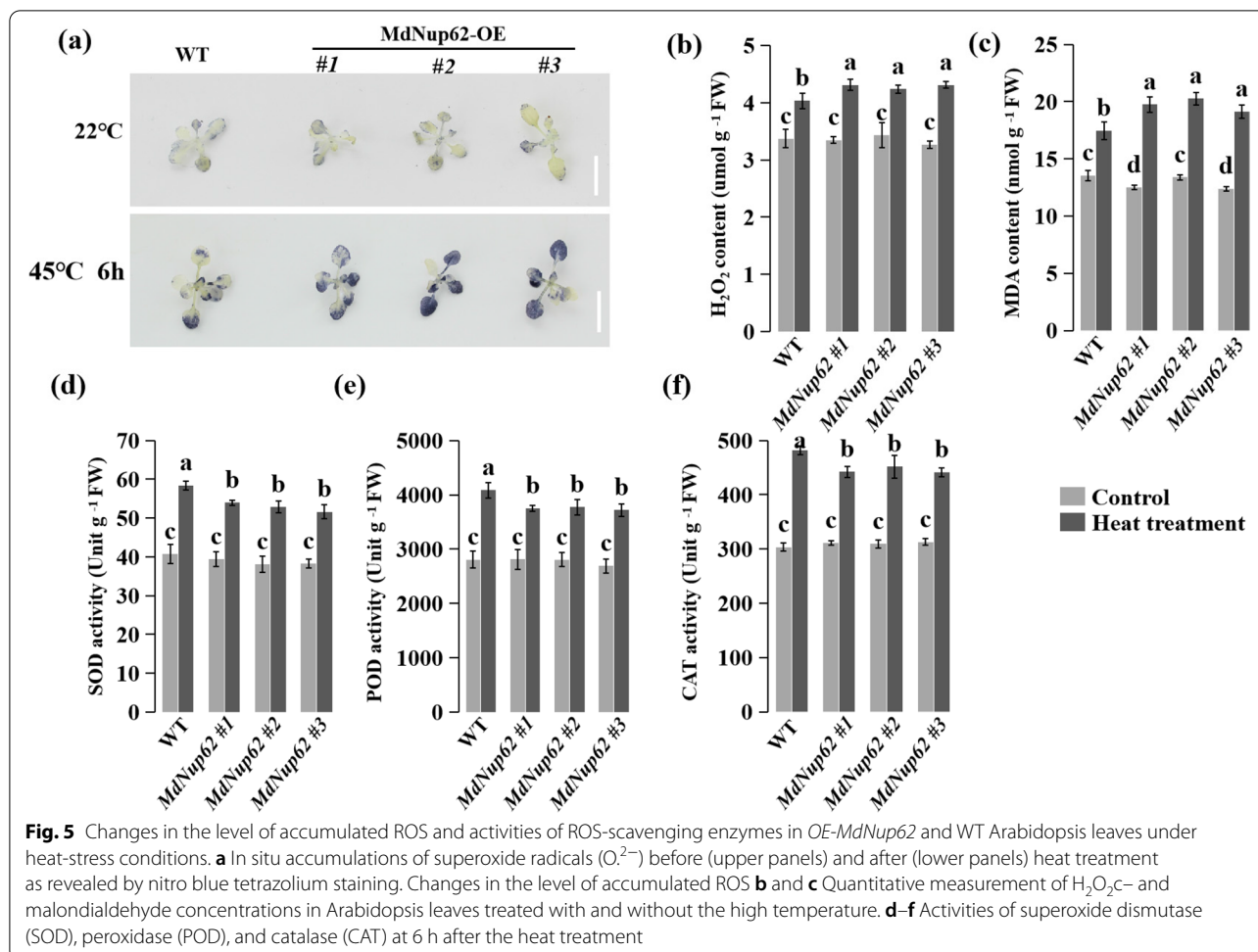
MdNup62* interacts with *MdHSFs

We cloned parts of the *MdHSFs* (*MdHSFA1a/b/d/e* and *MdHSFA9a/b*) independently into the pGADT7 vector and then cotransformed each with *MdNUP62*⁵⁰⁸⁻⁶¹³-pGBKT7. *MdNup62* interacted with these *MdHSFs* (Fig. 7a). Additionally, we used *MdHSFA9b* in pull-down assays. The recombinant *MdNup62*-HIS fusion protein was purified with *MdHSFA9b*-GST, but not with GST alone (Fig. 7b). The split-LUC complementation assay revealed that the co-expression of *MdNup62*-NLUC

with *MdHSFA1d*-CLUC or *MdHSFA9b*-CLUC resulted in a higher LUC activity than the other combinations (Fig. 7c-e). These results confirmed the interaction between *MdNup62* and both *MdHSFA1D* and *MdHSFA9b*.

Feature, expression, and subcellular localization analyses of *MdHSFA9b* and *MdHSFA1d*

Phylogenetic tree analysis showed that Apple and Arabidopsis HSFs were divided into four groups (I, II, III, IV), with *MdHSFA1a/b/d/e* in groupII, and *MdHSFA9a/b* in groupI (Fig. 8a). We also examined the expression patterns of *MdHSFs* in different tissues of several apple



varieties (Fig. 8b; Table S2). And the expression levels of *MdHSFA1a/b/d/e*.

and *MdHSFA9a/b* showed significantly higher in buds.

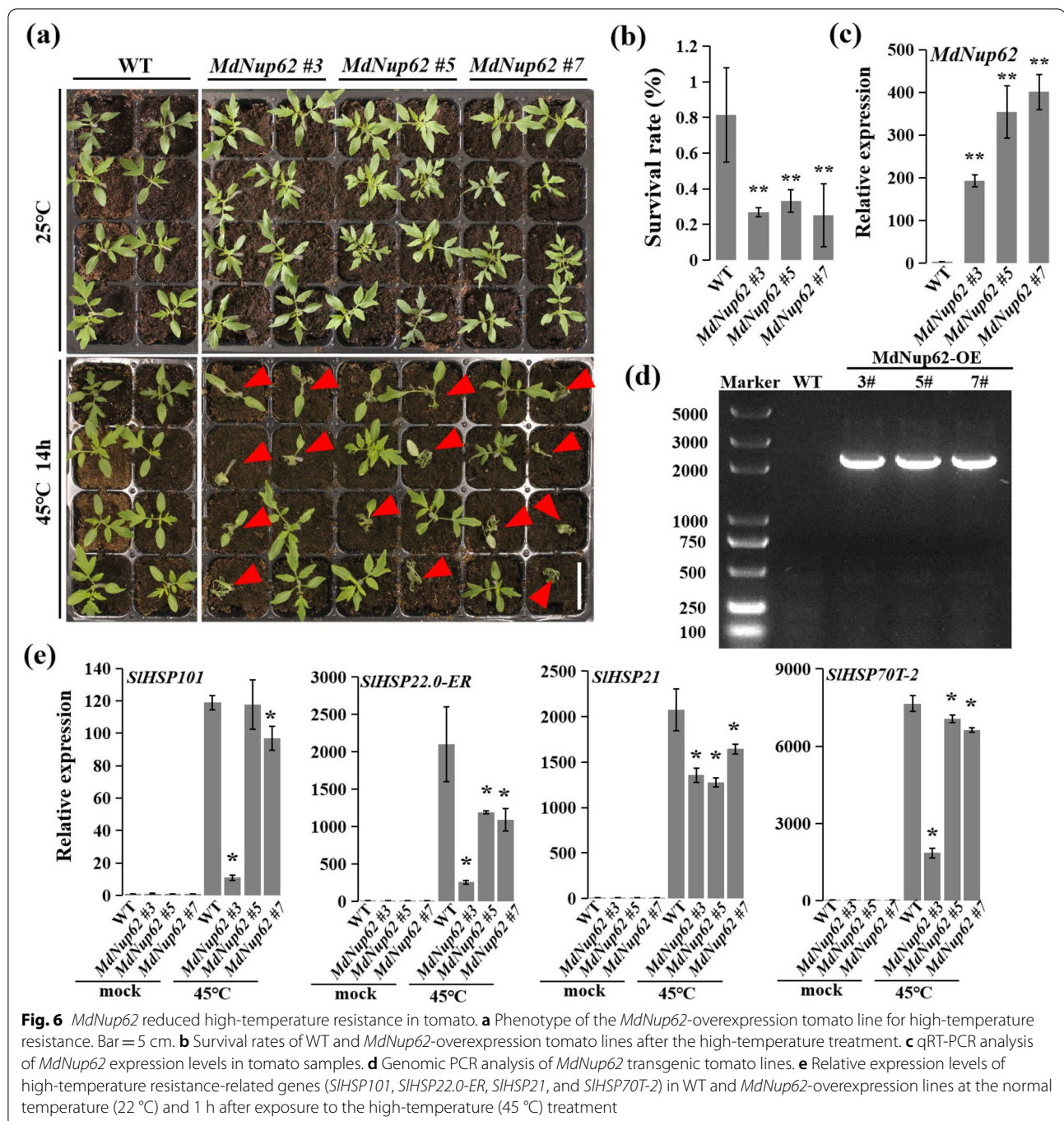
The subcellular localizations of *MdHSFA9b* and *MdHSFA1d* were studied by independently introducing 35S::*MdHSFA9b*-EGFP and 35S::*MdHSFA1d*-EGFP, respectively, into tobacco leaves (Fig. 8c). Tobacco leaves transformed with the empty vector 35S::EGFP served as controls. In the tobacco leaves expressing 35S::*MdHSFA9b*-EGFP and 35S::*MdHSFA1d*-EGFP, the GFP signals were observed in both the nucleus and cytoplasm, while the GFP signal was detected throughout the control tobacco leaf cells, indicating that *MdHSFA9b* and *MdHSFA1d* localized to both the nucleus and cytoplasm.

A tissue-specific expression analysis revealed that *MdHSFA1d* was expressed highest in flower buds and stems. The highest expression level of *MdHSFA9b* was in stems, but the expression levels in the other tissues were also high. Subsequently, the expression levels of *MdHSFA9b* and *MdHSFA1d* remained high during the

flower bud developmental stages, while the highest was at 70 days after flowering (Fig. 8d). These results indicated that *MdHSFA9b* and *MdHSFA1d* maintained high expression levels during flower bud induction, suggesting that they may be involved in the bud differentiation of apple.

Overexpression of *MdHSFA9b* and *MdHSFA1d* promotes flowering

To verify the flowering phenotype of HSFs, we performed Agrobacterium-mediated genetic transformations of *MdHSFA9b* and *MdHSFA1d* into *A. thaliana*. Like OE-*MdNup62*, OE-*MdHSFA9b* and OE-*MdHSFA1d* lines flowered significantly earlier than WT (Figs. 9a and S3a). Additionally, they also had significantly fewer rosette leaves than WT during bolting (Figs. 9b and S3b). We also performed genomic PCR (Figure S2b, c), semi-quantitative RT-PCR (Figs. 9c and S3c), and qRT-PCR (Figs. 9d and S3d) to confirm the presence of the transgene in the OE-*MdHSFA9b* and OE-*MdHSFA1d*

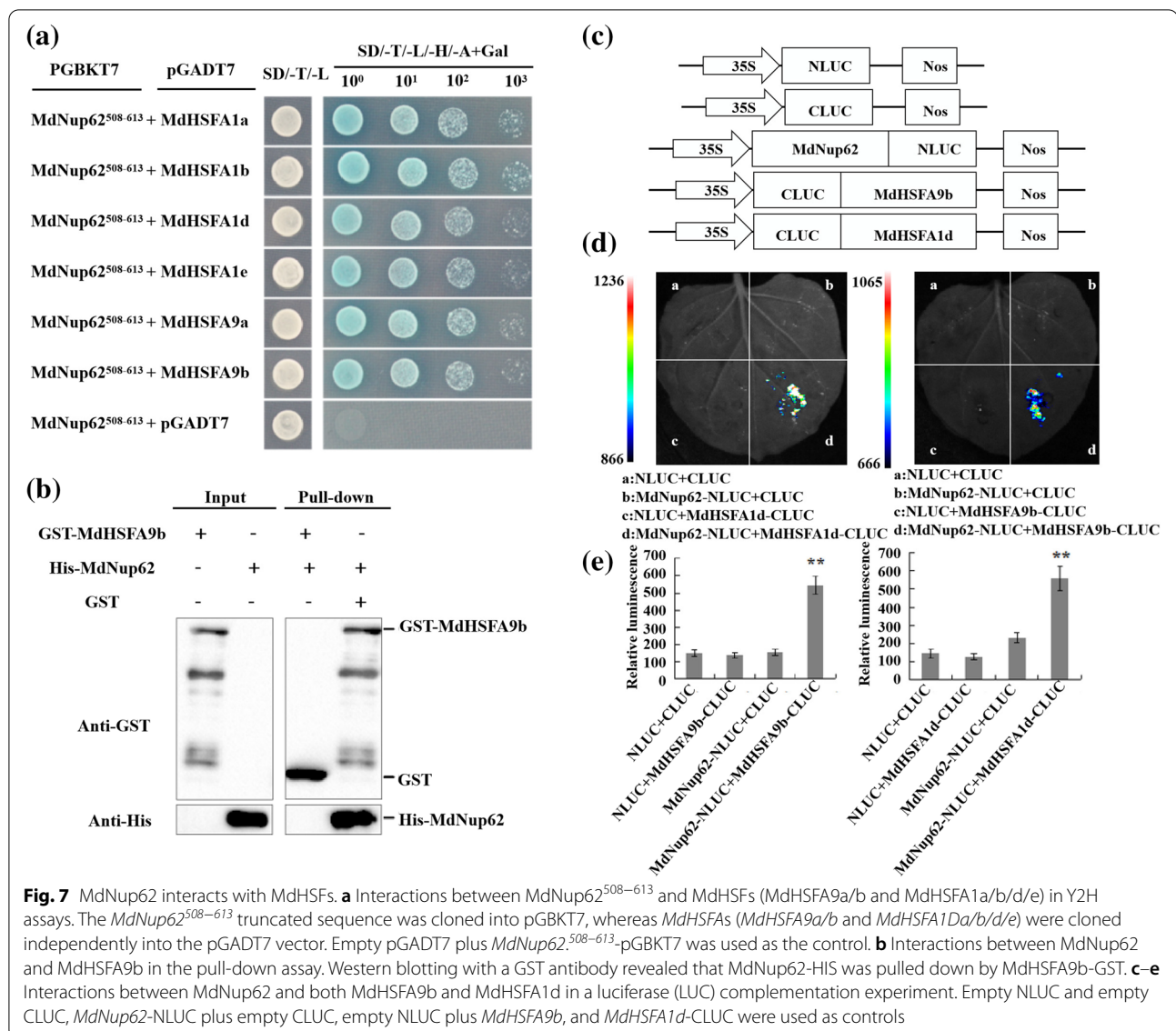


lines. The transcript levels of *AtFT*, *AtLFY*, and *AtSOC1* were significantly increased in OE-*MdHSEA9b* and OE-*MdHSEA1d* lines compared with WT (Figs. 9e and S3e).

Overexpression of *MdHSEA9b* and *MdHSEA1d* enhances high-temperature resistance

To study the high-temperature resistance phenotypes of *MdHSEA9b* and *MdHSEA1d*, we also exposed

OE-*MdHSEA9b* and OE-*MdHSEA1d* transgenic plants, respectively, to high-temperature (45 °C) conditions (Figs. 10a and S4a). The survival rates of OE-*MdHSEA9b* and OE-*MdHSEA1d* lines were significantly greater than that of WT (Figs. 10b and S4b). Consistently, the ROS accumulation in leaves decreased in transgenic plants after the high-temperature treatment (Figure S5a, b). We also performed a qRT-PCR



analysis of *A. thaliana* HSPs (*AtHSP101*, *AtHSP22-ER*, *AtHSP21.0*, and *AtHSP70T-2*) (Figs. 10c and S4c), and their expression levels in transgenic *A. thaliana* increased under high-temperature conditions compared with under normal growth conditions. These results indicated that *MdHSEA9b* and *MdHSEA1d* enhance plant high-temperature resistance.

Discussion

Plant flowering has always been an important topic in crop and horticultural sciences, and issues with apple flowering have long hindered the development of the apple industry in China [1, 2]. The Nups control protein transport between the nucleus and cytoplasm, and they participate in a variety of biological processes, including

flowering [19, 20]. In *A. thaliana*, Nup96 promotes the stability of HOS1, and HOS1 conjugates and degrades CO, then promotes *FLC* expression, leading to delayed flowering. In addition, HOS1 increases the stability of Nup96 and thus maintains this regulatory pathway to control the flowering time [23, 26]. Mutations in *Nup54*, *Nup58*, *Nup62*, *Nup136*, and *Nup160* have resulted in a prominent earlier flowering phenotype compared with WT [16, 25]. In the present study, *MdNup62* maintained a high expression level during flower development. To verify the flowering function of *MdNup62*, we determined the flowering phenotypes of OE-*MdNup62* *A. thaliana* lines. Interestingly, the phenotypes of the overexpression lines were consistent with Arabidopsis deletion mutants and showed obvious early flowering.

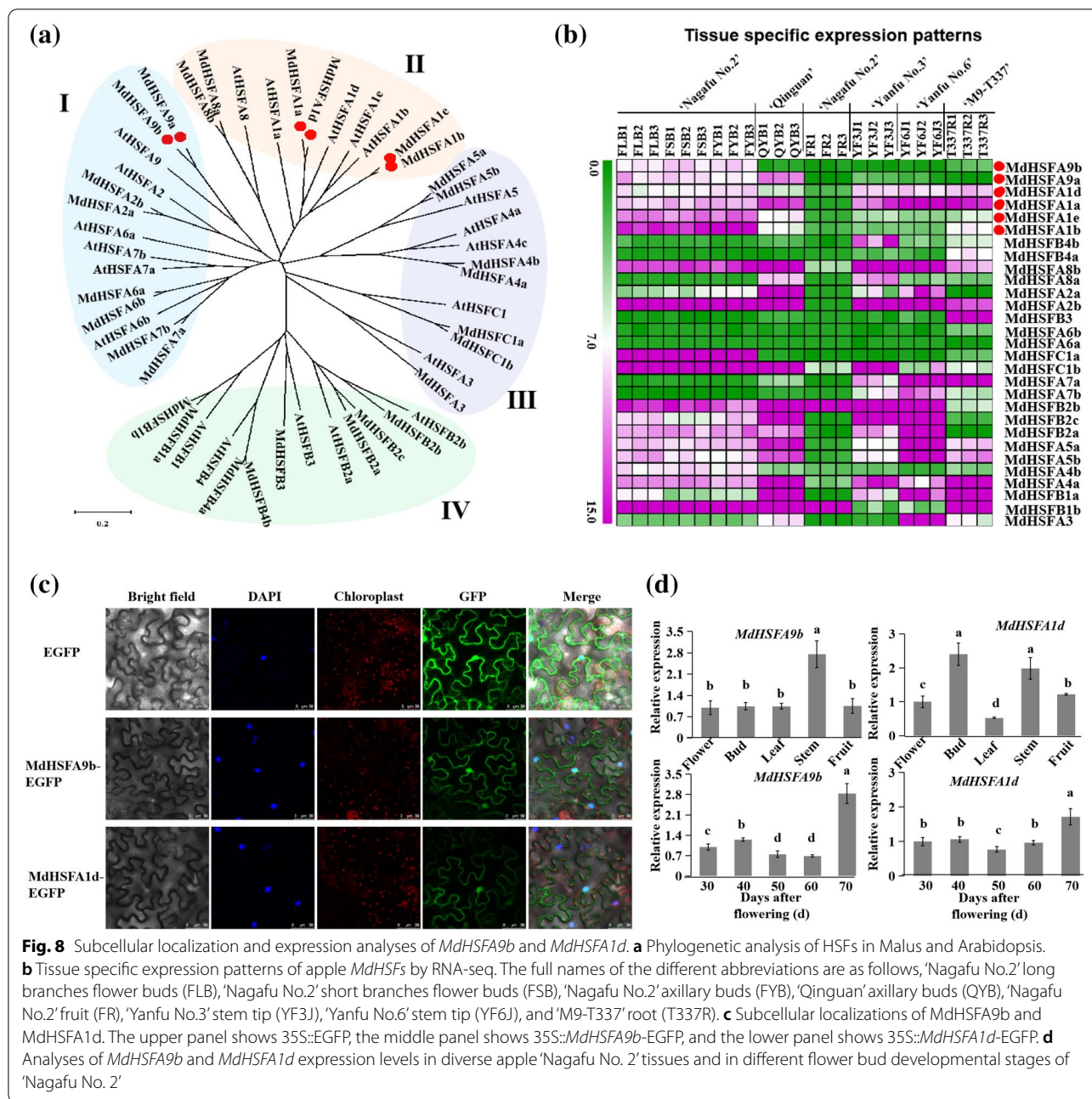


Fig. 8 Subcellular localization and expression analyses of *MdHSA9b* and *MdHSA1d*. **a** Phylogenetic analysis of HSFs in Malus and Arabidopsis. **b** Tissue specific expression patterns of apple *MdHSA*s by RNA-seq. The full names of the different abbreviations are as follows, 'Nagafu No.2' long branches flower buds (FLB), 'Nagafu No.2' short branches flower buds (FSB), 'Nagafu No.2' axillary buds (FYB), 'Qinguan' axillary buds (QYB), 'Nagafu No.2' fruit (FR), 'Yanfu No.3' stem tip (YF3J), 'Yanfu No.6' stem tip (YF6J), and 'M9-T337' root (T337R). **c** Subcellular localizations of *MdHSA9b* and *MdHSA1d*. The upper panel shows 35S::EGFP, the middle panel shows 35S::MdHSA9b-EGFP, and the lower panel shows 35S::MdHSA1d-EGFP. **d** Analyses of *MdHSA9b* and *MdHSA1d* expression levels in diverse apple 'Nagafu No. 2' tissues and in different flower bud developmental stages of 'Nagafu No. 2'

Previous studies found that both *Nup62* deletion mutants and overexpression strains of Arabidopsis have increased the sensitivities to auxin, indicating that the overexpression does not result in a functional gain, but rather a functional loss, like the mutant [51]. Therefore, the overexpression of *MdNup62* in this study may also result in a functional loss. However, *MdNup62* is involved in the flowering pathway.

With global warming, extreme high-temperatures will occur more frequently, which will seriously affect the

normal growth and development of plants [5, 6]. And *Nups* are involved in temperature-stress responses. *HOS1* and *Nup160* were reported to be involved in cold resistance [27, 28]. *Nup85* and *Nup133* control mRNA output only under warm conditions and are more sensitive to transcription factor localization at warm temperatures [20]. In this study, *MdNup62* responded to high-temperature stress in apple. However, OE-*MdNup62* lines had reduced high-temperature resistance in both Arabidopsis and tomato. By analysing the relative expression levels

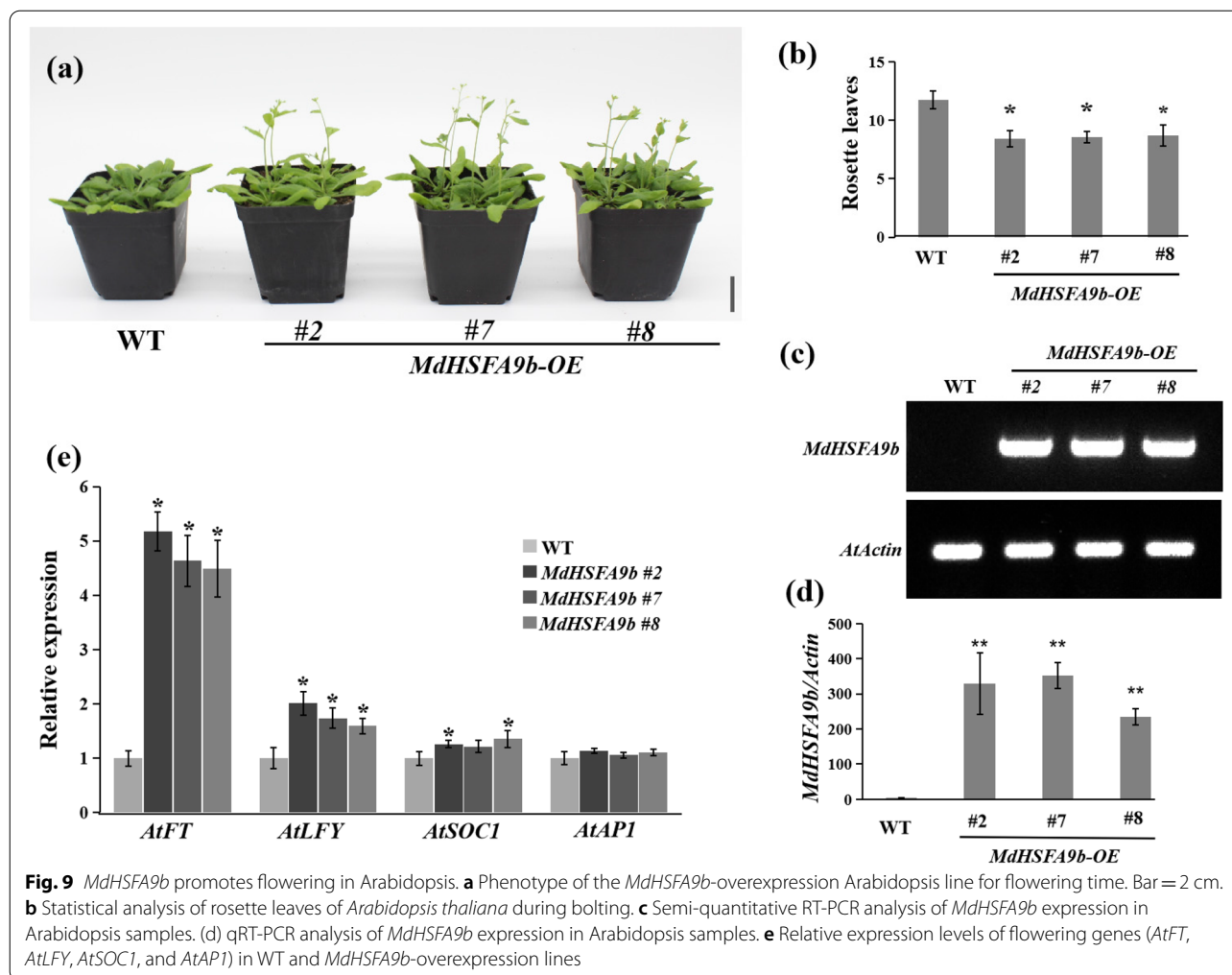


Fig. 9 *MdHSA9b* promotes flowering in Arabidopsis. **a** Phenotype of the *MdHSA9b*-overexpression Arabidopsis line for flowering time. Bar = 2 cm. **b** Statistical analysis of rosette leaves of *Arabidopsis thaliana* during bolting. **c** Semi-quantitative RT-PCR analysis of *MdHSA9b* expression in Arabidopsis samples. **d** qRT-PCR analysis of *MdHSA9b* expression in Arabidopsis samples. **e** Relative expression levels of flowering genes (*AtFT*, *AtLFY*, *AtSOC1*, and *AtAPI*) in WT and *MdHSA9b*-overexpression lines

of HSPs (*HSP101*, *HSP22-ER*, *HSP21.0*, and *HSP70T-2*) in transgenic plants, we found no obvious correlations between OE-*MdNup62* lines and WT at a normal growth temperature, but OE-*MdNup62* lines had significantly lower HSP expression levels than WT under high-temperature conditions.

In plants, Nup-interacting proteins have been studied [17, 18, 26], and some potential Nup85-interacting proteins have been identified by immunoprecipitation and subsequent mass spectrometry in Arabidopsis, such as the Nup107–160 subcomplex (Nup160, Nup133, Nup43, Nup96, Nup107, Seh1, and Sec13), several mediator subunits (MED16, MED14, and MED18), HOS1, and Sec13A. The interactions between Nup85 and three proteins, HOS1, Sec13A, and MED18, have been confirmed. Additionally, a direct interaction between Nup96 and HOS1 in Arabidopsis has also been reported [26]. In our previous study, the interaction between MdNup54 and MdNup62 was confirmed in apple [17]. However, there are no reports of direct interactions between

transcription factors and Nups in plants. We previously identified an interaction between apple MdNup54 and MdKNAT4/6 using a yeast double-hybridization test, but further verification is needed [17]. In this study, we verified direct interactions between MdNup62 and MdHSFs, indicating that the Nups may directly recognize related transcription factors and thus regulate their transport. This provides a new direction of study for Nups.

Because of the early flowering of OE-*MdNup62* Arabidopsis lines, MdHSFs that interact with MdNup62 may be also involved in the flowering pathway. Consistent with this conjecture, some HSFs are associated with flowering [49, 50]. HSA1E and HSA4C directly target and positively regulate the flowering gene *SOC1* in lettuce [49]. Arabidopsis HSA2 directly targets and promotes the expression of *REF6*, and the *REF6*–*HSA2* loop directly targets and activates *HTT5*, which coordinates early flowering [50]. In this study, we found that *MdHSA9b* and *MdHSA1d* maintained high expression levels during flower bud induction. Additionally,

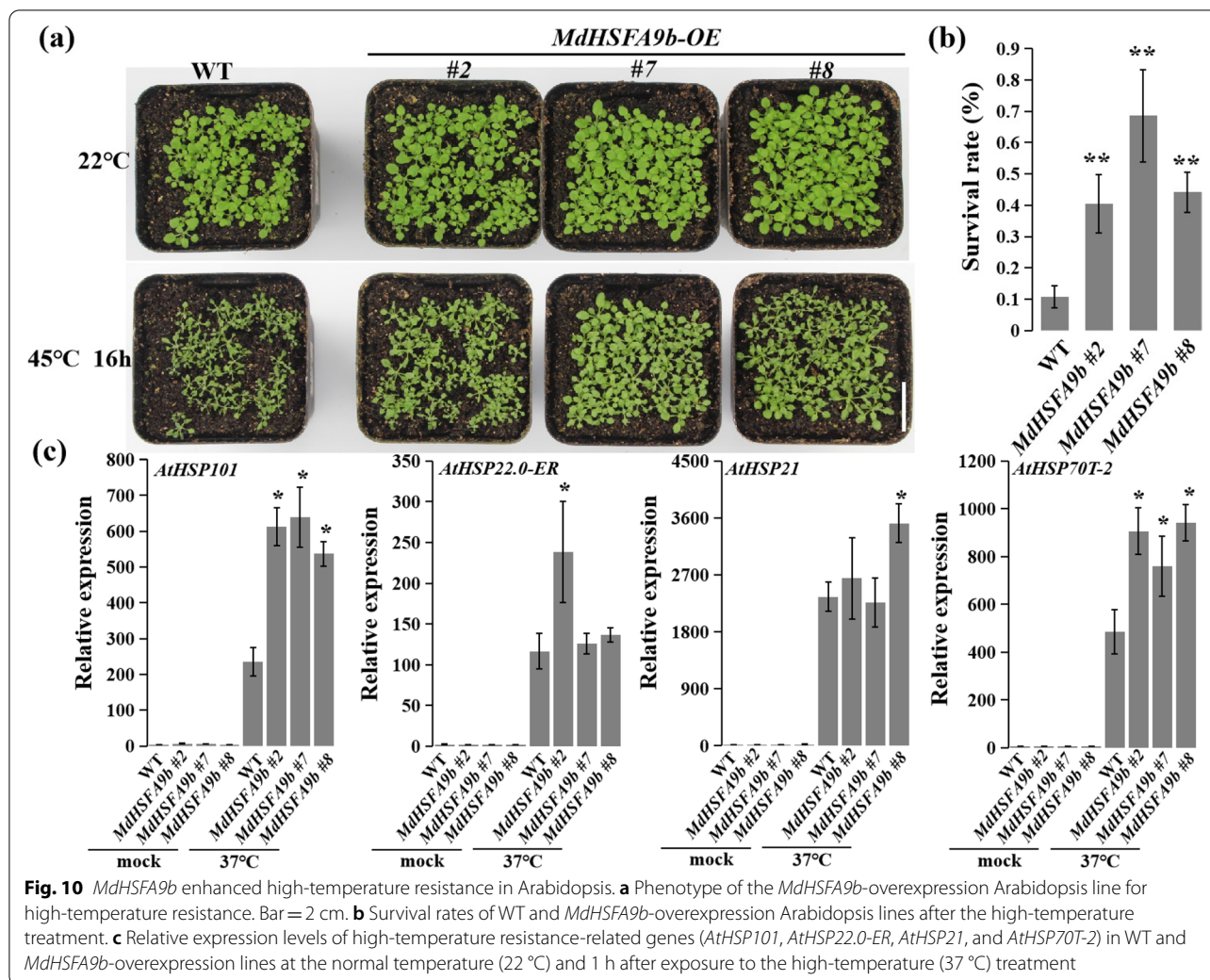
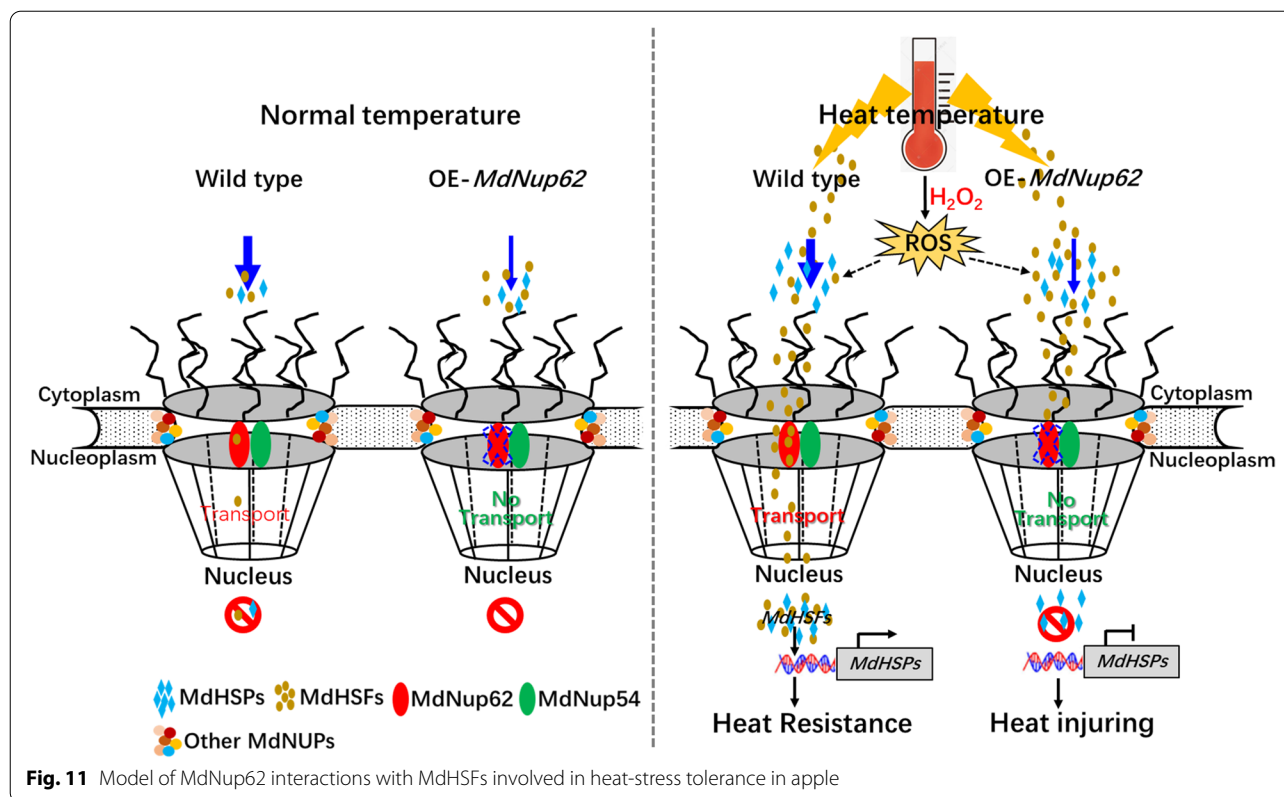


Fig. 10 *MdHSA9b* enhanced high-temperature resistance in Arabidopsis. **a** Phenotype of the *MdHSA9b*-overexpression Arabidopsis line for high-temperature resistance. Bar = 2 cm. **b** Survival rates of WT and *MdHSA9b*-overexpression Arabidopsis lines after the high-temperature treatment. **c** Relative expression levels of high-temperature resistance-related genes (*AtHSP101*, *AtHSP22.0-ER*, *AtHSP21*, and *AtHSP70T-2*) in WT and *MdHSA9b*-overexpression lines at the normal temperature (22 °C) and 1 h after exposure to the high-temperature (37 °C) treatment

OE-*MdHSA9b* and OE-*MdHSA1d* Arabidopsis lines flower significantly earlier than WT. This suggests that *MdHSA9b* and *MdHSA1d* promote plant flowering. *MdNup62*, *MdHSA9b*, and *MdHSA1d* share the same flowering phenotype, possibly because the overexpression of *MdNup62* fosters HSF accumulation in the nucleus, promoting the expression of downstream flowering-related genes and advancing flowering.

HSFs play important roles in regulating plant resistance to high temperatures. *HSA1* positively regulates the heat tolerance of tomato, the expression of *HSA2* is dependent on *HsfA1*, and the thermotolerance of the posttranscriptional silencing of the *HsfA1* gene in protoplasts can be restored by plasmid-borne *HsfA2* [52]. *HSA1d* and *HSA1e* activate *HsfA2* transcription, and a double knockout of *HSA1d* and *HSA1e* impairs tolerance to heat-shock stress [43]. In *Medicago truncatula*, *HSA9* plays important roles in thermotolerance [53]. In the current study, we obtained similar results for *MdHSA9b*

and *MdHSA1d*. The expression levels of *HSPs* in the two overexpression Arabidopsis lines were significantly greater than in WT, and both lines had enhanced high-temperature resistance levels. Like the flowering and auxin phenotypes [51], the opposite phenotypes between OE-*MdNup62* and OE-*MdHSA9b*, OE-*MdHSA1d* indicates that the overexpression of *MdNup62* may also result in a lack of function under heat-stress conditions. Similar to the results of this study, Zhang et al. (2020) found that *nup85* and *nup133* increase the ubiquitous protoplast (nucleus and cytosol) signals of IAA17 and PIF4 at 28 °C compared with at 22 °C. Furthermore, the *nup96* and *hos1* mutants show significant increases in the ubiquitous localizations of IAA17 and PIF4 signals at 28 °C (72% and 66%, respectively) compared with 22 °C (40% and 49%, respectively) [20]. Thus, the nuclear accumulations of the IAA17 and PIF4 proteins in *nup85*, *nup96*, *nup133*, and *hos1* are reduced compared with WT, and the defects are more severe at 28 °C. Therefore, we hypothesized



that the transport of MdHSFA9b, MdHSFA1d, and other MdHSFs is inhibited in OE-*MdNup62* lines at high temperatures, resulting in the inhibition of the transcription of downstream *HSPs*, which further reduces high-temperature resistance.

On the basis of these findings, we constructed a hypothetical model of *MdNup62*-related pathways involved in high-temperature resistance (Fig. 11). At normal temperature, apple *MdHSFs* were not induced, and not much transported into nucleus that cannot lead to up-regulate expression of *MdHSPs* in WT and OE-*MdNup62*. However, at high temperature, apple *MdHSFs* were significantly induced, and then transported into the nucleus through NPC channels to promote the expression of *MdHSPs* in WT, in which enhanced high-temperature resistance. But for OE-*MdNup62* lines, the structure of the apple NPC changed, and blocked the transport of high temperature induced MdHSFs into the nucleus that cannot induce much *MdHSPs* expression causing heat injuring (Fig. 11). Additionally, OE-*MdNup62*, OE-*MdHSFA9b* and OE-*MdHSFA1d* lines showed significant early flowering phenotype compared with WT (Fig. 3, 9; Figure S3).

In conclusion, temperature is an important factor affecting flowering. With global warming, apple flowering will occur earlier, increasing the risk of chilling-related injury. Moreover, extreme hot weather is also

occurring frequently. Both climatic conditions seriously affect the development of the apple industry. *MdNup62* interacts with *MdHSFs* to regulate flowering and heat-resistance pathways in plants. Thus, both *MdNup62* and the *MdHSFs* regulate flowering and respond to temperature changes. This research provides a theoretical reference for managing the impact of global warming on the apple industry.

Materials and methods

Plant materials and growth conditions

The plant materials were 6-year-old apple trees ('Fuji' / T337/*Malus robusta* Rehd.) growing in the experimental orchard of the Horticulture College of Northwest A & F University (108°04' E, 34°16' N). We collected new shoots (2–3 mm in diameter) near the tips, fully expanded leaves near buds, flower buds, blooming flowers, and young fruit, which were immediately frozen in liquid nitrogen and stored at -80°C for later use.

The 'Fuji' plants were grown on MS medium containing $0.1\text{ mg}\cdot\text{L}^{-1}$ indolebutyric acid and $0.6\text{ mg}\cdot\text{L}^{-1}$ 6-benzylaminopurine under long-day conditions (16 h-light/8 h-dark) at 24°C and were subcultured every 45 days. Arabidopsis plants ('Columbia') were grown under long-day conditions (16 h-light/8 h-dark) at 22°C . Tomato plants ('Ailsa Craig') were grown under long-day

conditions (16 h-light/8 h-dark) at 25 °C. And the arabidopsis and tomato seeds were previously preserved in our laboratory.

Heat map, protein alignment, and phylogenetic analysis

Based on RNA-seq data of our laboratory, the heat map of apple different tissues was constructed using MeV (Multiple Experiment Viewer) software. A protein sequence alignment of Nup62 from six Rosaceae plants was performed using DNAMAN software. The Nup62 protein sequences were obtained from the GDR database (<https://www.rosaceae.org/>). The phylogenetic tree was constructed using MEGA-X software.

RNA extraction and qRT-PCR analysis

Total RNA was extracted from apple trees, Arabidopsis seedlings, tomato seedlings, and apple seedlings using an RNA Plant Plus Reagent Kit (TIANGEN, Beijing, China). The RNA was used as the template to synthesize cDNA with a PrimeScript RT Reagent Kit (Takara, Shiga, Japan). The qRT-PCR analysis was conducted on a StepOnePlus Real-Time PCR System (Thermo Fisher Scientific, USA). The reaction solution contained 10 µL SYBR Green I Master Mix (CWBI, Beijing, China), 0.5 µmol·L⁻¹ primers (SANGON BIOTECH, Shanghai, China), and 1 µL each template in a total volume of 20 µL. The PCR program was as follows: 95 °C for 3 min; 40 cycles of 94 °C for 15 s, 60 °C for 20 s, and 72 °C for 15 s. All the samples were analysed with three biological replicates, each comprising three technical replicates. Relative gene expression levels were calculated in accordance with the 2^{-ΔΔCt} method [54]. The primers used for qRT-PCR (Table S4) were synthesized by the Sangon Biotechnology Co. Ltd. (Shanghai, China).

Subcellular localization

The open reading frames (ORFs) of the *MdNup62*, *MdHSFA1d*, and *MdHSFA9b* genes were inserted independently into the pCAMBIA2300-EGFP vector to generate the 35S::*MdNup62*-EGFP, 35S::*MdHSFA1d*-EGFP, and 35S::*MdHSFA9b*-EGFP recombinant plasmids, respectively. These recombinant plasmids were inserted independently into *Agrobacterium tumefaciens* strain GV3101 cells. The GV3101 cells containing these recombinant plasmids were then infiltrated into tobacco leaves. GV3101 cells containing the pCAMBIA2300-EGFP vector (35S::EGFP) served as the control. After an additional 3 days of growth in the dark, green fluorescent protein (GFP) signals in transformed tobacco leaves were detected using a Leica TCS SP8 SR Laser Scanning Confocal Microscope (Leica, Germany). The primers used are listed in Table S5.

Genetic transformation

The genetic transformations were performed in accordance with published methods for Arabidopsis [55] and tomato ('Ailsa Craig') [56] plants. The transgenic Arabidopsis and tomato lines were selected on MS plates supplemented with 50 mg·L⁻¹ and 100 mg·L⁻¹ kanamycin, respectively.

Yeast two-hybrid (Y2H) assay

The *MdNup62*^{508–613} truncated sequence was cloned into the pGBKT7 vector to generate the *MdNup62*^{508–613}-pGBKT7 recombinant plasmid. The *MdHSFAs*' ORFs were inserted individually into the pGADT7 vector to generate the *MdHSFAs*-pGADT7 recombinant plasmids. The recombinant plasmids were inserted into Gold Yeast Two-Hybrid cells, which were then grown on a selective medium. The primers used are listed in Table S5.

Split luciferase (LUC) complementation

The full-length *MdHSFA1d* and *MdHSFA9b* coding sequences were cloned independently into the CLUC vector, while *MdNup62* was cloned into the NLUC vector. The split-LUC complementation assay was performed with tobacco leaves. The reconstituted LUC activity was detected in the dark using a Princeton Lumazine Pylon 2048B cooling camera (Princeton, USA). The LUC activity was quantified using the Dual-Luciferase Reporter Assay System (Promega, USA). The primers used are listed in Table S5.

Pull-down assays

The ORFs of *MdNup62* and *MdHSFA9b* were cloned into the pET-28a and pGEX-6p-1 vectors, respectively, and subsequently overexpressed independently in *Escherichia coli* BL21(DE3) (Transgene). The pull-down assays were conducted using the His-Tagged Protein Purification Kit (Clontech) in accordance with the manufacturer's instructions. The primers used are listed in Table S5.

Heat-tolerance assays

The 'Fuji' plants at 30 days after propagation were used for the 45 °C heat treatment. We collected leaf samples before and at 1, 3, and 6 h after the treatment. The samples were immediately frozen in liquid nitrogen and stored at -80 °C for later use.

Two-week-old transgenic Arabidopsis and 3-week-old transgenic tomato were used for the heat treatment in an artificial climate chamber. OE-*MdNup62* *A. thaliana* lines were subjected to 45 °C for 12 h, and OE-*MdHSFA9b* and OE-*MdHSFA1d* *A. thaliana* lines were subjected to 45 °C for 16 h. OE-*MdNup62* tomato lines were subjected to 45 °C for 14 h.

Evaluation of stress tolerance

The superoxide dismutase, peroxidase, and catalase activities and the malondialdehyde and H₂O₂ levels were detected using the corresponding Suzhou Comin Biotechnology test kits (Suzhou Comin Biotechnology Co., Ltd, Suzhou, China). The presence of O²⁻ in leaf samples was determined by staining with nitro blue tetrazolium.

Statistical analyses

Statistical analyses were performed using SPSS software. Data are reported as means ± SDs. Asterisks (*) indicate significant differences between treatments as assessed by Student's t-test at $P < 0.05$ (*) and $P < 0.01$ (**). Different lowercase letters above the bars indicate significant differences ($P < 0.05$, Tukey's test).

Abbreviations

HSF: Heat shock factor; MS: Murashige and skoog; NPC: Nuclear pore complex; OE: Overexpression; ORF: Open reading frame; PCR: Polymerase chain reaction; qRT-PCR: Quantitative real-time PCR; ROS: Reactive oxygen species; WT: Wild type.

Supplementary Information

The online version contains supplementary material available at <https://doi.org/10.1186/s12870-022-03698-3>.

Additional file 1: Table S1. Expression of NPC components in different tissues of several apple varieties. **Table S2.** Expression of *MdHSFs* in different tissues of several apple varieties. **Table S3.** *MdNup62* yeast double-hybridization screening results. **Table S4.** Primers used for qRT-PCR. **Table S5.** Primers used for plasmid construction. **Figure S1.** Interactions between *MdNup62* and *MdNup54* in *aluciferase* (LUC) complementation experiment. **Figure S2.** Genomic PCR analyses of *MdNup62* (a), *MdHSFA9b* (b), and *MdHSFA1d* (c) in transgenic *Arabidopsis* lines. **Figure S3.** *MdHSFA1d* promotes flowering in *Arabidopsis*. **Figure S4.** *MdHSFA1d* enhanced high-temperature resistance in *Arabidopsis*. **Figure S5.** Changes in the levels of accumulated ROS in *Arabidopsis* leaves under heat-stress conditions. **Figure S6.** Schematic diagram of vector. **Figure S7.** Original image of nucleic acid electrophoresis. **Figure S8.** Original image of Figure 7b.

Acknowledgements

The authors thank all contributors for their work and would like to thank the reviewers for their valuable comments and suggestions.

Authors' contributions

Libo Xing and Chenguang Zhang conceived and designed the experiment. Chenguang Zhang, Peng Jia, Na An, Wei Zhang, Jiayan Liang, Hua Zhou performed the experiment. Dong Zhang, Juanjuan Ma, Caiping Zhao, Mingyu Han, Xiaolin Ren, Chenguang Zhang and Peng Jia analyzed the data. Chenguang Zhang and Libo Xing wrote the manuscript. The author(s) read and approved the final manuscript.

Funding

This work was financially supported by the National Natural Science Foundation of China (31801813; 32072522); the China Postdoctoral Science Foundation (2018M631207, 2017M623254); Natural Science Foundation of Shaanxi Province (2020JQ-248).

Availability of data and materials

All data generated or analysed during the current study are available in this article and its supplementary information files. Gene sequences can be downloaded at NCBI database (<https://www.ncbi.nlm.nih.gov/>). And the GenBank

accession number of *MdNup62* is MT102240, *MdHSFA9a* is ON364334, *MdHSFA9b* is ON364335, *MdHSFA1a* is ON364336, *MdHSFA1b* is ON364337, *MdHSFA1d* is ON364338, *MdHSFA1e* is ON364339, and *MdNup54* is MT102239.

Declarations

Ethics approval and consent to participate

Prior to conducting the research, the permission from Horticulture College of Northwest A & F University to collect and analyse the 'Fuji' apple sample documented in this work was obtained. All the experimental materials in this study do not violate the IUCN Policy Statement on Research Involving Species at Risk of Extinction and Convention on the Trade in Endangered Species of Wild Fauna and Flora, and have been approved by the government.

Consent for publication

Not applicable.

Competing interests

The authors declare that the research was conducted in the absence of any commercial or financial relationships that could be construed as a potential conflict of interest.

Received: 11 August 2021 Accepted: 30 May 2022

Published online: 04 July 2022

References

- Fan S, Zhang D, Lei C, Chen H, Xing L, Ma J, et al. Proteome analyses using iTRAQ labeling reveal critical mechanisms in alternate bearing *malus prunifolia*. *J Proteome Res*. 2016;15(10):3602–16.
- Guitton B, Kelner J, Velasco R, Gardiner SE, Chagné D, Costes E. Genetic control of biennial bearing in apple. *J Exp Bot*. 2012;63(1):131–49.
- Romanovskaja D, Bakšienė E. Influence of climatic warming on beginning of flowering of apple tree (*Malus domestica* Borkh.) in Lithuania. *Agron Res*. 2009;7(1):87–96.
- Liu L, Guo L, Li M, Fu W, Luan Q, et al. Changes of chilling and heat accumulation of apple and their effects on the first flowering date in the main planting areas of northern China. *Chin J Appl Ecol*. 2020;31(7):2457–63.
- Zhou B, Sun J, Liu W, Zhang Q, Wei. Dwarfing apple rootstock responses to elevated temperatures: A study on plant physiological features and transcription level of related genes. *J Integr Agr*. 2016;15(5):1025–33.
- Yao F, Song C, Wang H, Song S, Jiao J, Wang M, et al. Genome-wide characterization of the HSP20 gene family identifies potential members involved in temperature stress response in apple. *Front Genet*. 2020;11:609184.
- Bäurle I, Dean C. Timing of Developmental Transitions in Plants. *Cell*. 2006;125(4):655–644.
- Komeda Y. Genetic regulation of time to flower in *Arabidopsis thaliana*. *ANNU REV PLANT BIOL*. 2004;55(1):521–35.
- Teotia S, Tang G. To bloom or not to bloom: role of MicroRNAs in plant flowering. *MOL PLANT*. 2015;8(3):359–77.
- Kotoda N, Wada M, Kusaba S, Kano-Murakami Y, Masuda T, Soejima J. Overexpression of *MdMADS5*, an APETALA1-like gene of apple, causes early flowering in transgenic *Arabidopsis*. *Plant Sci (Limerick)*. 2002;162(5):679–87.
- Kotoda N, Iwanami H, Takahashi S, Abe K. Antisense expression of *MdTFL1*, a TFL1-like gene, reduces the juvenile phase in apple. *J AM SOC HORTIC SCI*. 2006;131(1):74–81.
- Xing L, Zhang D, Li Y, Shen Y, Zhao C, et al. Transcription profiles reveal sugar and hormone signaling pathways mediating flower induction in apple (*Malus domestica* Borkh.). *PLANT CELL PHYSIOL*. 2015;56(10):2052–68.
- Liu K, Feng S, Pan Y, Zhong J, Chen Y, Yuan C, et al. Transcriptome analysis and identification of genes associated with floral transition and flower development in sugar apple (*Annona squamosa* L.). *Front Plant Sci*. 2016;7:1695.
- Li Y, Zhang D, An N, Fan S, Zuo X, Zhang X, et al. Transcriptomic analysis reveals the regulatory module of apple (*Malus x domestica*) floral transition in response to 6-BA. *BMC Plant Biol*. 2019;19(1):93.

15. Zhang S, Gottschalk C, van Nocker S. Genetic mechanisms in the repression of flowering by gibberellins in apple (*Malus x domestica* Borkh.). *BMC Genomics*. 2019;20(1):747.
16. Tamura K, Fukao Y, Iwamoto M, Haraguchi T, Hara-Nishimura I. Identification and characterization of nuclear pore complex components in *Arabidopsis thaliana*. *Plant Cell*. 2010;22(12):4084–97.
17. Zhang C, An N, Zhang W, Zhang X, et al. Genomic identification and expression analysis of nuclear pore proteins in *Malus domestica*. *Sci Rep-Uk*. 2020;10(1):17426.
18. Zhu Y, Wang B, Tang K, Hsu CC, Xie S, Du H, et al. An *Arabidopsis* nucleoporin NUP85 modulates plant responses to ABA and salt stress. *Plos Genet*. 2017;13(12):e1007124.
19. Parry G. Assessing the function of the plant nuclear pore complex and the search for specificity. *J Exp Bot*. 2013;64(4):833–45.
20. Zhang A, Wang S, Kim J, Yan J, Yan X, Pang Q, et al. Nuclear pore complex components have temperature-influenced roles in plant growth and immunity. *Plant Cell Environ*. 2020;43(4):1452–66.
21. Xu XM, Meier I. The nuclear pore comes to the fore. *Trends Plant Sci*. 2008;13(1):20–7.
22. Yang Y, Wang W, Chu Z, Zhu J, Zhang H. Roles of nuclear pores and nucleocytoplasmic trafficking in plant stress responses. *Front Plant Sci*. 2017;8:574.
23. Lazaro A, Mouriz A, Piñeiro M, Jarillo JA. Red light-mediated degradation of CONSTANS by the E3 ubiquitin ligase HOS1 regulates photoperiodic flowering in *Arabidopsis*. *Plant Cell*. 2015;27(9):2437–54.
24. Jung JH, Park JH, Lee S, To TK, Kim JM, Seki M, et al. The cold signaling attenuator High expression of ostomatically responsive gene1 activates flowering locus C transcription via chromatin remodeling under short-term cold stress in *Arabidopsis*. *The Plant Cell*. 2013;25(11):4378–90.
25. Parry G. Components of the *Arabidopsis* nuclear pore complex play multiple diverse roles in control of plant growth. *J Exp Bot*. 2014;65(20):6057–67.
26. Cheng Z, Zhang X, Huang P, Zhu J, Chen F, et al. Nup96 and HOS1 are mutually stabilized and gate CONSTANS protein level, conferring long-day photoperiodic flowering regulation in *Arabidopsis*. *The Plant Cell*. 2020;32(2):374–91.
27. Ishitani M, Xiong L, Lee H, Stevenson B, Zhu JK. HOS1, a genetic locus involved in cold-responsive gene expression in *Arabidopsis*. *Plant Cell*. 1998;10(7):1151–61.
28. Dong CH, Agarwal M, Zhang Y, Xie Q, Zhu JK. The negative regulator of plant cold responses, HOS1, is a RING E3 ligase that mediates the ubiquitination and degradation of ICE1. *Proc Natl Acad Sci PNAS*. 2006;103(21):8281–6.
29. Dong CH, Hu X, Tang W, Zheng X, Kim YS, Lee BH, et al. A putative *Arabidopsis* nucleoporin, AtNUP160, is critical for RNA export and required for plant tolerance to cold stress. *Mol Cell Biol*. 2006;26(24):9533–43.
30. Cheng YT, Germain H, Wiermer M, Bi D, Xu F, García AV, et al. Nuclear pore complex component MOS7/Nup88 is required for innate immunity and nuclear accumulation of defense regulators in *Arabidopsis*. *The Plant Cell*. 2009;21(8):2503–16.
31. Zhang Y, Li X. A putative nucleoporin 96 is required for both basal defense and constitutive resistance responses mediated by suppressor of npr1–1, constitutive 1. *The Plant Cell*. 2005;17(4):1306–1316.
32. Roth C, Wiermer M. Nucleoporins Nup160 and Seh1 are required for disease resistance in *Arabidopsis*. *Plant Signal Behav*. 2012;7(10):1212–4.
33. Robles LM, Deslauriers SD, Alvarez AA, Larsen PB. A loss-of-function mutation in the nucleoporin AtNUP160 indicates that normal auxin signalling is required for a proper ethylene response in *Arabidopsis*. *J Exp Bot*. 2012;63(5):2231–41.
34. Parry G, Ward S, Cernac A, Dharmasiri S, Estelle M, et al. The *Arabidopsis* suppressor of auxin resistance proteins are nucleoporins with an important role in hormone signaling and development. *Plant Cell*. 2006;18(7):1590–603.
35. Jacob Y, Mongkolsiriwatana C, Veley KM, Kim SY, Michaels SD. The nuclear pore protein AtTPR is required for RNA homeostasis, flowering time, and auxin signaling 1[C][W][OA]. *Plant Physiol (Bethesda)*. 2007;144(3):1383–90.
36. Xu XM, Rose A, Muthuswamy S, Jeong SY, Venkatakrishnan S, Zhao Q, et al. Nuclear pore anchor, the *Arabidopsis* homolog of Tpr/Mlp1/Mlp2/megator, is involved in mRNA export and SUMO homeostasis and affects diverse aspects of plant development. *Plant Cell*. 2007;19(5):1537–48.
37. Wiermer M, Cheng YT, Imkampe J, Li M, Wang D, Lipka V, et al. Putative members of the *Arabidopsis* Nup107–160 nuclear pore sub-complex contribute to pathogen defense. *Plant J*. 2012;70(5):796–808.
38. Scharfa K, Berberich T, Ebersberger I, Nover L. The plant heat stress transcription factor (Hsf) family: Structure, function, and evolution. *Biochim Biophys Acta*. 2012. <https://doi.org/10.1016/j.bbagr.2011.10.002>.
39. Nover L, Bharti K, Doring P, Mishra SK, Ganguli A, Scharf KD. *Arabidopsis* and the heat stress transcription factor world: how many heat stress transcription factors do we need? *Cell Stress Chaperones*. 2001;6(3):177–89.
40. Wang N, Liu W, Yu L, Guo Z, Chen Z, Jiang S, et al. Heat shock factor A8a modulates flavonoid synthesis and drought tolerance. *Plant Physiol*. 2020;184(3):1273–90.
41. Kotak S, Port M, Ganguli A, Bicker F, von oskull-Döring P. Characterization of C-terminal domains of *Arabidopsis* heat stress transcription factors (Hsfs) and identification of a new signature combination of plant class A Hsfs with AHA and NES motifs essential for activator function and intracellular localization. *Plant J*. 2004;39(1):98–112.
42. Littlefield O, Nelson HCM. A new use for the “wing” of the “winged” helix-turn-helix motif in the HSF-DNA cocystal. *Nat Struct Mol*. 1999;6(5):464–70.
43. Nishizawa-Yokoi A, Nosaka R, Hayashi H, Tainaka H, Maruta T, Tamoi M, et al. HsfA1d and HsfA1e involved in the transcriptional regulation of HsfA2 function as key regulators for the Hsf signaling network in response to environmental stress. *Plant Cell Physiol*. 2011;52(5):933–45.
44. Schramm F, Larkindale J, Kiehlmann E, Ganguli A, Englich G, Vierling E, et al. A cascade of transcription factor DREB2A and heat stress transcription factor HsfA3 regulates the heat stress response of *Arabidopsis*. *Plant J*. 2008;53(2):264–74.
45. Qian J, Chen J, Liu YF, Yang LL, Li WP, Zhang LM. Overexpression of *Arabidopsis* HsfA1a enhances diverse stress tolerance by promoting stress-induced Hsp expression. *Genet Mol Res*. 2014;13(1):1233–43.
46. Tian X, Wang F, Zhao Y, Lan T, Yu K, Zhang L, et al. Heat shock transcription factor A1b regulates heat tolerance in wheat and *Arabidopsis* through OPR3 and jasmonate signalling pathway. *Plant Biotechnol J*. 2020;18(5):1109–11.
47. Chang Y, Liu H, Liu N, Chi W, Wang C, Chang S, et al. A heat-inducible transcription factor, HsfA2, is required for extension of acquired thermotolerance in *Arabidopsis*. *Plant Physiol*. 2007;143(1):251–62.
48. Ikeda M, Mitsuda N, Ohme-Takagi M. *Arabidopsis* HsfB1 and HsfB2b Act as repressors of the expression of heat-inducible Hsfs but positively regulate the acquired thermotolerance 1[C][W][OA]. *Plant Physiol*. 2011;157(3):1243–54.
49. Chen Z, Zhao W, Ge D, Han Y, Ning K, Luo C, et al. CM-seq reveals the crucial role of *LSOC1* in heat-promoted bolting of lettuce (*Lactuca sativa* L.). *Plant J*. 2018;95(3):516–28.
50. Liu J, Feng L, Gu X, Deng X, Qiu Q, Li Q, et al. An H3K27me3 demethylase-HSF2 regulatory loop orchestrates transgenerational thermomemory in *Arabidopsis*. *Cell Res*. 2019;29(5):379–90.
51. Boeglin M, Fuglsang AT, Luu DT, Sentenac H, Gaillard I, Chereil I. Reduced expression of AtNUP62 nucleoporin gene affects auxin response in *Arabidopsis*. *BMC Plant Biol*. 2016;16:2.
52. Mishra SK. In the complex family of heat stress transcription factors, HsfA1 has a unique role as master regulator of thermotolerance in tomato. *Gene Dev*. 2002;16(12):1555–67.
53. Zinsmeister J, Berriri S, Basso DP, Ly Vu B, Dang TT, Lalanne D, et al. The seed-specific heat shock factor A9 regulates the depth of dormancy in *Medicago truncatula* seeds via ABA signalling. *Plant Cell Environ*. 2020;43(10):2508–22.
54. Livak KJ, Schmittgen TD. Analysis of Relative Gene Expression Data Using Real-Time Quantitative PCR and the 2^{-ΔΔCT} Method. *Methods*. 2001;25(4):402–8.
55. Clough SJ, Bent AF. Floral dip: a simplified method for *Agrobacterium*-mediated transformation of *Arabidopsis thaliana*. *Plant J*. 1998;16(6):735–43.
56. Liu DD, Sun XS, Liu L, Shi HD, Chen SY, Zhao DK. Overexpression of the Melatonin Synthesis-Related Gene SLCOMT1 Improves the Resistance of Tomato to Salt Stress. *Mol*. 2019;24(8):1514.

Publisher's Note

Springer Nature remains neutral with regard to jurisdictional claims in published maps and institutional affiliations.